Spectral diffusion dephasing and motional narrowing in single semiconductor quantum dots

Guillaume CASSABOIS

Abstract In this review, we address the extrinsic dephasing mechanism of spectral diffusion that dominates the decoherence in semiconductor quantum dots at cryogenic temperature. We discuss the limits of random telegraph and Gaussian stochastic noises, and we describe the general effect of motional narrowing in the context of spectral noise. We emphasize the unconventional phenomenology of motional narrowing in standard semiconductor quantum dots at low incident power and temperature, that makes the quantum dot emission line a sensitive probe of the extrinsic reservoir fluctuation dynamics. We further show that the text book phenomenology of motional narrowing in nuclear magnetic resonance is recovered in quantum dots embedded in field-effect heter-ostructure. In that case, the electrical control of the mesoscopic environment of the quantum dot leads to conventional motional narrowing where the motion consists in carrier tunneling out of the defects around the quantum dot.

1 Introduction

The application of single semiconductor quantum dots (QDs) in quantum information devices is tightly related to the QD decoherence dynamics and to its impact on the device efficiency. In single photon sources, the broadening of the QD emission line beyond the natural linewidth does not restrict the use of these nanostructures [1], whereas it raises severe limitations in the prospect of indistinguishable photon generation [2, 3], or qu-bit coherent manipulation [4]. One of the most prominent features of QDs, and more generally of solid-state nanostructures investigated for

Guillaume CASSABOIS
Ecole Normale Supérieure, Laboratoire Pierre Aigrain, 24 rue Lhomond 75231 Paris Cedex 5, France, e-mail: guillaume.cassabois@lpa.ens.fr
Université Montpellier 2, 34095 Montpellier Cedex 5, France, e-mail: guillaume.cassabois@ges.univ-montp2.fr

quantum information application, is the strong modification of the decoherence dynamics with the temperature of the surrounding matrix. In semiconductor QDs at room temperature, the decoherence is governed by the intrinsic interaction with acoustic phonons and by the subsequent appearance of lateral phonon side-bands in the optical spectrum. More precisely, the coupling to a continuum of acoustic phonons leads to an emission spectrum that consists in a central zero-phonon line with lateral sidebands, that dominate the optical spectrum at room temperature [5]. On the contrary, at low temperature, the QD matrix contributes to the decoherence dynamics through the extrinsic process of spectral diffusion. Photoluminescence experiments in single QDs have revealed that the QD environment generates fluctuating electric fields and shifts the QD line through the quantum confined Stark effect. This so-called spectral diffusion phenomenon was interpreted as due to carriers randomly trapped in defects, impurities in the QD vicinity [6, 7, 8]. This phenomenon with spectral jitters ranging from few tens of μeV to several meV breaks down the simple picture of a two-level system for which the optical line would be given at low temperature by the radiative limit in the μeV range.

In this paper, we review the extrinsic dephasing mechanism of spectral diffusion in semiconductor QDs. In Section 2, we first present the theoretical framework that allows a comprehensive description of spectral diffusion. In the two limit cases of random telegraph and Gaussian stochastic noises, we discuss the existence of two fluctuation regimes: the slow modulation one where the QD optical spectrum directly reflects the statistical distribution of the QD emission energy, and the fast modulation one, also called motional narrowing regime, where the QD line is a Lorentzian with a width smaller than the standard deviation of the QD energy. In Section 3, we illustrate the rich phenomenology of spectral diffusion dephasing in semiconductor QDs by first showing the experimental evidence for a smooth transition between the two fluctuation regimes. In standard QDs, the motional narrowing regime strikingly occurs in the limit of low temperature or low incident power, in contrast to the text book example of nuclear magnetic resonance. In a second example, we show that motional narrowing can be controlled by a dc-gate voltage for a QD embedded in a field-effect hetero-structure. In that case, we observe tunneling-assisted motional narrowing where the motion consists in the tunneling of carriers out of the defects located in the QD mesoscopic environment. The conventional phenomenology of nuclear magnetic resonance is thus recovered and opens the way for a protection of zero-dimensional electronic states from outside coupling.

2 Theory

The optical spectrum of a two-level system perturbed by frequency fluctuation was addressed by Kubo in his seminal paper on the stochastic theory of lineshape and relaxation [9]. The central point is the calculation of the so-called relaxation function $\phi(t)$ which corresponds to the Fourier transform of the intensity spectrum, and which quantifies the accumulated phase because of the random frequency fluctua-

tion $\delta\omega(t)$ around a mean value ω_0 [9]:

$$\phi(t) = \left\langle \exp\left(i \int_0^t \delta\omega(u)du \right) \right\rangle \quad (1)$$

where $\langle ... \rangle$ denotes the average over different configurations.

Under the assumption of a Markovian modulation, the frequency fluctuation is conveniently analyzed within a model based on a Markov chain composed of an arbitrary number of N independent random telegraphs, as detailed below.

2.1 Random telegraph noise

A random telegraph is a two-state jump process that corresponds to a discrete spectral shift $\delta\omega = \pm\Omega/2$ of the optical line. The transition from the upper (lower) state to the lower (upper) one occurs with a probability $dt/\tau_\downarrow$ ($dt/\tau_\uparrow$) in the time interval dt and induces a spectral jump $-\Omega$ ($+\Omega$), as sketched in Fig. 1. In the context of spectral diffusion in QDs, the upper (lower) state corresponds to an empty (occupied) defect, $\tau_\downarrow$ ($\tau_\uparrow$) to the capture (escape) time of one carrier in the defect, and Ω to the Stark shift of the QD line due to the electric field created by the charge carrier in the defect located in the QD vicinity.

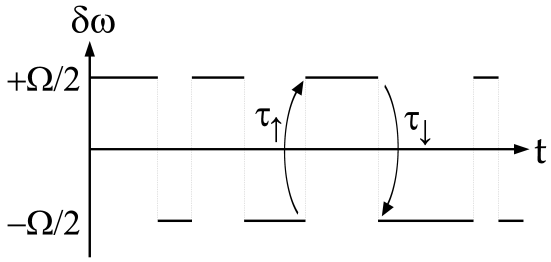

Fig. 1 Frequency fluctuation of the QD emission line as a function of time in the presence of a single random telegraph. Ω is the Stark shift of the QD line due to the electric field created by the charge carrier in the defect located in the QD vicinity. $\tau_\downarrow$ and $\tau_\uparrow$ are the characteristic time constants of the jump processes.

The relaxation function $\phi_1(t)$ of a single random telegraph was calculated by Wódkiewicz *et al.* in the case of symmetric jump processes ($\tau_\downarrow = \tau_\uparrow$ in Fig. 1) [10]. In the prospect of a more general theory that would catch the specific physics of semiconductor nanostructures, the former model has been extended to the case of asymmetric two-state jump processes and the expression of the relaxation function $\phi_1(t)$ has been derived when $\tau_\uparrow \neq \tau_\downarrow$ [11]. Following the guidelines of the Kubo theory, the generalized analytical expression of the relaxation function $\phi_1(t)$ reads:

$$\phi_1(t) = G_{+1}(t) - G_{-1}(t) \quad (2)$$

with

$$G_\varepsilon(t) = \frac{1+\varepsilon Y + i\eta X}{2Y} \exp\left[-(1-\varepsilon Y)\frac{|t|}{2\tau_c}\right] \quad (3)$$

where the correlation time τ_c is given by $\frac{1}{\tau_c}=\frac{1}{\tau_\uparrow}+\frac{1}{\tau_\downarrow}$, $\eta=\frac{\tau_\uparrow-\tau_\downarrow}{\tau_\uparrow+\tau_\downarrow}$ characterizes the intensity asymmetry in the emission spectrum, $X=\Omega\tau_c$, and Y is given by $Y^2=1-X^2+2i\eta X$ with the condition $\Re(Y)\geq 0$. In the simple case of symmetric jump processes (η=0), one easily recovers for $\phi_1(t)$ the expression given in Ref [10].

If $\Omega\tau_c \gg 1$, the system is in the so-called slow modulation limit. By taking the Fourier transform of Eq. (2) for η=0, one gets a symmetric doublet structure for the optical spectrum, with two lines split by Ω and a full width at half maximum $1/\tau_c$. In other words, when $\Omega\tau_c \gg 1$, the optical spectrum reflects the statistical distribution corresponding to Fig. 1, with a line-broadening given by the fluctuating rate $1/\tau_c$. For asymmetric jump processes, the optical spectrum exhibits an asymmetric doublet where the ratio of the integrated intensity of the two separate lines is given by $\frac{1-\eta}{1+\eta}$.

In the fast modulation limit or motional narrowing regime ($\Omega\tau_c \ll 1$), the reduction of the accumulated phase induces the spectral coalescence of the two lines and the doublet structure disappears [9]. The spectrum transforms from a doublet with a splitting Ω to a single Lorentzian line with a width given by the product $\Omega * \frac{\Omega\tau_c}{2}$, thus meaning that the shorter the correlation time, the narrower the line compared to the splitting Ω.

2.2 Gaussian stochastic noise

In his pioneering work [9], Kubo analyzed the opposite situation where the frequency fluctuation is characterized by a Gaussian probability density, thus corresponding to a large number of random telegraphs ($N \gg 1$). The derivation of the relaxation function $\phi_{G_N}(t)$ for a Gaussian stochastic noise brought the general theoretical framework for the interpretation of various experiments, and in particular the motional narrowing effect observed in nuclear magnetic resonance [12].

In their pre-Gaussian noise theory, Wódkiewicz *et al.* made the link between random telegraphs and Gaussian stochastic processes by calculating the relaxation function $\phi_N(t)$ for a given number of N identical random telegraphs. Under the assumption of uncorrelation for the random telegraphs, the relaxation function $\phi_N(t)$ reads $[\phi_1(t)]^N$, and when $N \gg 1$, the relaxation function $\phi_N(t)$ converges to the one obtained for a Gaussian noise $\phi_{G_N}(t)$ [10]:

$$\phi_{G_N}(t) = \exp\left[-\Sigma^2\tau_c^2\left(\exp\left(-\frac{|t|}{\tau_c}\right)+\frac{|t|}{\tau_c}-1\right)\right] \quad (4)$$

which is a consequence of the central limit theorem in the context of spectral noise. The parameter Σ in Eq.(4) is the standard deviation of the QD frequency, and in the simple case of symmetric jump processes ($\tau_\uparrow$=$\tau_\downarrow$), Σ is given by $\frac{\sqrt{N}\Omega}{2}$ [10].

In order to complete the generalization of the spectral diffusion theory and address the case of Gaussian stochastic processes with asymmetric jump events, the general expression of Σ has been derived when $\tau_\uparrow \neq \tau_\downarrow$, and the expression of the frequency modulation amplitude Σ reads [13]:

$$\Sigma = \frac{\sqrt{N}\Omega}{\sqrt{\frac{\tau_\uparrow}{\tau_\downarrow}} + \sqrt{\frac{\tau_\downarrow}{\tau_\uparrow}}} \tag{5}$$

which reaches its maximum value $\Sigma_s = \frac{\sqrt{N}\Omega}{2}$ when $\tau_\uparrow = \tau_\downarrow$ and vanishes in the limit of strong asymmetric jump processes ($\tau_\uparrow \gg \tau_\downarrow$ or $\tau_\uparrow \ll \tau_\downarrow$).

If $\Sigma\tau_c \gg 1$, the system is in the slow modulation limit, in analogy to the single random telegraph phenomenology described above. The relaxation function has a Gaussian decay so that the optical spectrum has a Gaussian profile that reflects the Gaussian distribution law of the spectral noise. The full width at half maximum depends solely on the frequency modulation amplitude and is given by $2\sqrt{2\ln 2}\Sigma$.

In the fast modulation limit $\Sigma\tau_c \ll 1$, the relaxation function dynamics is strongly modified by motional narrowing, and it is characterized by an exponential decay. In the Fourier domain, the optical spectrum corresponds to a Lorentzian line with a width $2\Sigma^2\tau_c$, that is, the shorter the correlation time the narrower the optical spectrum.

In nuclear magnetic resonance, the transition from the slow modulation limit to the fast modulation one was observed on increasing the temperature [12]. This configuration corresponds to the particular case of symmetric jump processes ($\tau_\uparrow = \tau_\downarrow$) where the frequency modulation amplitude is constant with a value given by $\frac{\sqrt{N}\Omega}{2}$. As a matter of fact, the transition from $\Sigma\tau_c \gg 1$ to $\Sigma\tau_c \ll 1$ implies that τ_c decreases as a function of temperature, which is due to the thermal activation of the nuclei motion in nuclear magnetic resonance [9].

In the case of spectral diffusion in semiconductor QDs, we will see in Section 3 that the motional narrowing phenomenology is more complex because the frequency fluctuation dynamics is not restricted to the case of symmetric processes (η=0).

3 Experiments

We illustrate the various aspects of motional narrowing in semiconductor QDs by presenting measurements performed in self-assembled InAs/GaAs QDs grown by molecular beam epitaxy in the Stranski-Krastanow mode. The photoluminescence signal arising from a single QD is analyzed by means of Fourier-transform spectroscopy, which allows a high-resolution sampling of the Fourier-transform of the intensity spectrum on typically thousands of points [14]. This value is by two orders of magnitude larger than the average number of illuminated pixels in a charge-coupled device in the case of standard multi-channel detection in the spectral domain. The Fourier-transform technique is implemented in the detection part of the

setup where the photoluminescence signal passes through a Michelson interferometer placed in front of a grating spectrometer. The signal is detected by a low noise Si-based photon counting module. A translation stage varies the time t for propagation in one arm of the interferometer and one records interferograms of the photoluminescence emission $I(t)$=$I_0(1+C(t)\cos(\omega_0 t))$, where I_0 is the average photoluminescence signal intensity, ω_0 the central detection frequency, and $C(t)$ the interference contrast which corresponds to the modulus of the Fourier transform of the optical spectrum, i.e. with the notation above $C(t)$=$|\phi_N(t)|$. The implementation of this technique in single QD spectroscopy allows a precise determination of both width and shape of the emission line in order to accurately study the spectral diffusion phenomenon and the related QD decoherence.

3.1 Unconventional motional narrowing

We present in this section the experimental evidence for a crossover from the fast to the slow modulation limits. We show that a smooth transition between a Lorentzian line-profile and a Gaussian one is induced on increasing the incident power or the temperature for a QD in a simple heterostructure [13]. The existence of motional narrowing at low incident power or low temperature is a striking manifestation of the asymmetry of the jump processes for spectral diffusion in semiconductor QDs.

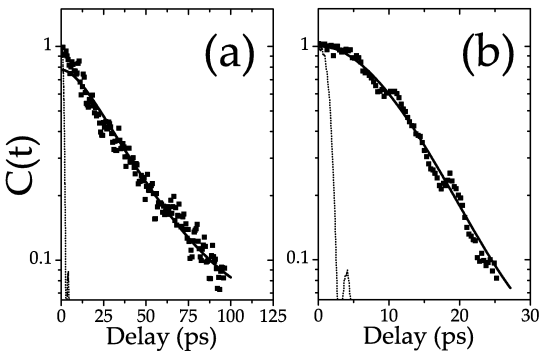

Fig. 2 Interferogram contrast $C(t)$ of the photoluminescence signal of a single InAs/GaAs quantum dot at 10K, on semi-logarithmic plots, for two different incident powers: 0.18 (a), and 2.88 kW.cm^{-2} (b). Data (squares), system response function (dotted line), theoretical fits (solid line) obtained by the convolution of the system response function with $\phi_{G_N}(t)$.

In Fig. 2 we display the measured (squares) interference contrast $C(t)$ for the emission spectrum of a single InAs/GaAs quantum dot at 10K, on semi-logarithmic plots, for two different incident powers: 0.18 (a) and 2.88 kW.cm^{-2} (b). We first observe that the coherence relaxation dynamics becomes faster for large incident powers. Moreover, there is an important modification in the decay of $C(t)$. At low power (Fig. 2(a)), the interference contrast decay is quasi-exponential with a time constant of 29 ps, thus corresponding to a quasi-Lorentzian profile with a full width at half maximum of 45 μeV. At higher power (Fig. 2(b)), the interference contrast

decay is predominantly Gaussian, thus corresponding to a quasi-Gaussian profile, with a full width at half maximum of 155 μeV.

A quantitative interpretation of the measurements is achieved by comparing the experimental data with the convolution of $\phi_{G_N}(t)$ (Eq. 4) with the system response function (dotted lines in Fig. 2) which is obtained under white light illumination. The calculated fits are displayed in solid line in Fig. 2 and an excellent agreement is reached with increasing values of $\Sigma\tau_c$ of 0.6 in (a), and 1.35 in (b). In Fig. 3(a) the whole set of values of $\Sigma\tau_c$ is displayed as a function of the excitation density, on a semi-logarithmic scale. This parameter characterizes the shape of the emission spectrum and the crossover from the exponential to the Gaussian decoherence dynamics occurs around $\Sigma\tau_c \sim 1$. Its gradual increase demonstrates the transition from the fast modulation limit to the slow modulation one when increasing the incident power. Similar results are obtained by means of temperature-dependent measurements where the transition from Lorentzian to Gaussian line-profiles occurs on increasing the temperature, with values of $\Sigma\tau_c$ as a function of the temperature displayed in Fig. 3(b). As a matter of fact, it shows that motional narrowing occurs for low excitation and low temperature.

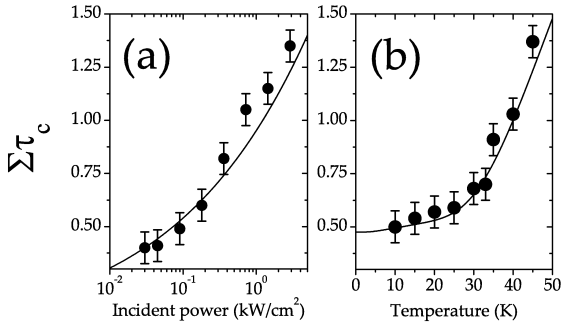

Fig. 3 Fitting parameter $\Sigma\tau_c$ versus incident power (a) and temperature (b). Data (symbols), and calculations (solid lines) are plotted as a function of incident power on a semi-logarithmic scale (a), and temperature (b).

The extracted values of $\Sigma\tau_c$ are confronted with calculations performed with Eq. (5), and a fair agreement is observed for the parameters $\hbar\Sigma_s \sim 400$ μeV, $\tau_\downarrow \sim 10$ ps, and $1/\tau_\uparrow = (1/\tau_0)\sqrt{P}$ in Fig. 3(a) where $\tau_0 \sim 1.6$ ns and P is in unit of 1 kW.cm^{-2} [13]. The asymmetry between the power dependences of $\tau_\downarrow$ and $\tau_\uparrow$ stems from the existence of different microscopic processes. The escape rate dependence on incident power is characteristic of Auger-type processes. In the elastic collision of two carriers where one is ejected from the trap while a delocalized carrier relaxes in energy, the escape rate is proportional to the density of delocalized carriers, which increases with incident power. As far as $\tau_\downarrow$ is concerned, the constant value of 10 ps stems from an optical-phonon assisted capture in the traps around the quantum dot [13]. For the temperature-dependent measurements (Fig. 3(b)), the escape rate varies with temperature according to $1/\tau_\uparrow = n_1(T)/\tau_1 + n_2(T)/\tau_2$ with $\tau_1 \sim 35$ ns, $\tau_2 \sim 10$ ps, $E_1 \sim 1$ meV, and $E_2 \sim 20$ meV, and where the Bose-Einstein occupation factor $n_i(t)$ given by $1/(\exp(E_i/kT)\text{-}1)$ accounts for the absorption of a phonon of mean energy E_i during the thermally-activated escape of the carriers out of the defects [13].

The asymmetry of the capture and escape mechanisms appears as the fundamental reason why motional narrowing strikingly occurs when decreasing the incident power or the temperature. If both processes had the same efficiency ($\tau_\uparrow$=$\tau_\downarrow$), one would have τ_c=$\tau_\uparrow/2$ and Σ=Σ_s, so that the spectral modulation amplitude would not depend on the time constant $\tau_\uparrow$. Therefore, the ratio $\Sigma\tau_c$ could only decrease when increasing the reservoir excitation. This situation corresponds to the well-known phenomenology in nuclear magnetic resonance where the activation of the nuclei motion induces the motional narrowing effect. In the present case where $\tau_\downarrow/\tau_\uparrow \leq 10^{-2}$, we are in the opposite regime where the correlation time is merely constant with relative variation smaller than 10^{-2} whereas the spectral modulation amplitude shows a steep increase with $\tau_\downarrow/\tau_\uparrow$ ($\Sigma \propto \sqrt{\tau_\downarrow/\tau_\uparrow}$). The ratio $\Sigma\tau_c$ thus increases when increasing the reservoir excitation with incident power or temperature. As a matter of fact, this non-standard phenomenology explains the observation of Lorentzian profiles in single QD spectroscopy with a width which is not given by the intrinsic radiative limit, but by the extrinsic reservoir fluctuation dynamics [15].

In the prospect of reducing the environment-induced decoherence in quantum information devices, the question then arises whether motional narrowing could be controlled by other parameters than incident power or temperature, in order to recover the conventional phenomenology of nuclear magnetic resonance and achieve an inhibition of dephasing.

3.2 Voltage-controlled conventional motional narrowing

Such a perspective was explored by embedding single QDs in a field-effect heterostructure in order to study the control of the spectral diffusion dynamics with a dc-gate voltage [11].

The sample consists of InGaAs QDs that are separated by a 25 nm GaAs layer from a highly n-doped GaAs substrate. The QDs are capped by 15 nm of GaAs, followed by a 75 nm AlGaAs blocking barrier and finally 60 nm of GaAs. After growth, a 10 nm thick semitransparent Ti Schottky contact was deposited on the top surface. In order to study single QDs, 400 nm diameter apertures are opened lithographically into a 200 nm thick Au mask [11]. By varying the gate voltage applied between the back and Schottky contacts, one can tune the QD electron states relative to the Fermi energy and thus control the electron occupation in the QDs in order to perform a high resolution study of the neutral exciton line as a function of the gate voltage.

In Fig. 4, we display the interferogram contrast $C(t)$ on semi-logarithmic plots, for the neutral exciton line at 30K for two gate voltages of -0.24 (a) and -0.2 V (b). These measurements reveal that the coherence decay at -0.24 V (Fig. 4(a)) is slower than at -0.2 V (Fig. 4(b)), and consequently that the linewidth decreases as a function of electric field with a total reduction of 20% in the whole bias range (Fig. 5(a)). These measurements are in strong contrast with the well known tunneling-assisted broadening observed in quantum wells, or in QDs in the regime of photo-current

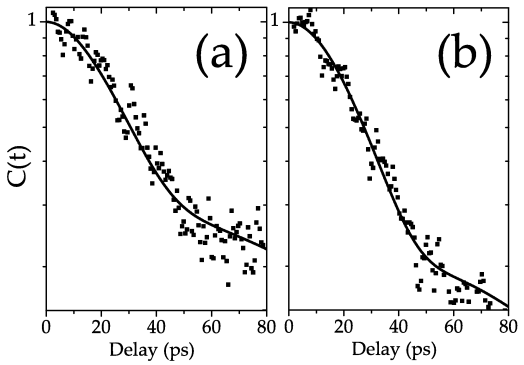

Fig. 4 Interferogram contrast $C(t)$ of the photoluminescence signal of a single InGaAs QD at 30K, on semi-logarithmic plots, for two gate voltages: -0.24 V (a), and -0.2 V (b). Data (squares), theoretical fits (solid line).

spectroscopy [16, 17]. In fact, the field-induced narrowing observed in Fig. 5(a) arises from the electrical control of spectral diffusion, and more precisely from motional narrowing assisted by tunneling.

A quantitative interpretation of these experimental data is reached in the framework of the pre-Gaussian noise theory [11]. The complex mesoscopic environment is described by a composite relaxation function where the $\phi_{G_N}(t)$ component (Eq. 4) depends on gate voltage through the escape time $\tau_\uparrow$. In Fig. 4, the calculated contrasts are displayed in solid line and an excellent agreement is obtained thus showing that the model accounts for the variation of the whole emission spectrum (shape and width) with gate voltage. More precisely, the complete set of data as a function of voltage and temperature is fitted by taking $\hbar\sqrt{N}\Omega$=56 μeV, $\tau_\downarrow$=45 ps, and by only varying $\tau_\uparrow$ with the values indicated in Fig. 5(b). The constant time $\tau_\downarrow$ (shown by a dashed line in Fig. 5(b)) is consistent with multi-phonon assisted capture in defects [18].

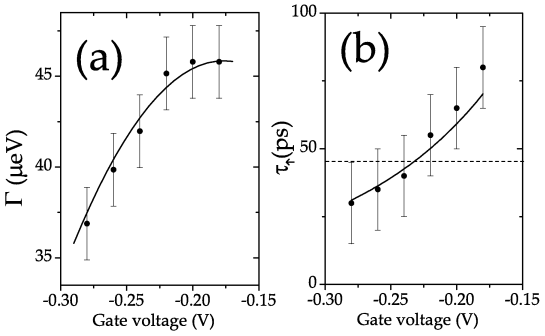

Fig. 5 (a) Linewidth versus gate voltage at 30K. Data (symbols), theoretical fits (solid line). (b) Tunneling time $\tau_\uparrow$ versus gate voltage. Data (symbols), theoretical fit (solid line). The horizontal line indicates the capture time $\tau_\downarrow$= 45 ps.

In Fig. 5(b), a systematic decrease of the escape time $\tau_\uparrow$ is observed with the reverse bias, as expected for field-induced tunneling. In analogy to the thermo-ionization of deep centers [19], these variations are interpreted by taking a phonon-assisted tunneling rate that is proportional to the transmission through a trian-

gular barrier due to a static electric field [19]. The data in Fig. 5(b) are reproduced by taking $\tau_\uparrow = \tau_\infty \top(F)^{-1}$ where $\top(F)$ is the barrier transmission given by $\exp\left(\frac{-4\sqrt{2m^* E_{io}^3}}{3\hbar eF}\right)$ with F the electric field strength along the growth direction, m^* the effective mass and E_i the effective ionization energy. We fit our data with E_{io}^e=245 meV in the case of electrons (m^*=0.07m_0) or E_{io}^h=145 meV for holes (m^*=0.34m_0), τ_∞=3.5$\times 10^{-5}$ps. The large values of E_{io} suggest that the spectral diffusers are deep defects, in agreement with the recent experimental evidence by deep level transient spectroscopy of the coexistence of deep levels with optically active InAs QDs [20].

This field-induced narrowing effect demonstrates the achievement of the text book phenomenology of nuclear magnetic resonance where the linewidth decreases by increasing the motion. In our solid-state system, the motion is tunneling controlled by a dc-gate voltage, and it induces an inhibition of dephasing in our single QD-device, that could be implemented in electrically-pumped single photon sources.

4 Conclusion

In this review, we have addressed the extrinsic dephasing mechanism of spectral diffusion that dominates the QD decoherence at cryogenic temperature. We have discussed the limits of random telegraph and Gaussian stochastic noises, and described the general effect of motional narrowing in the context of spectral noise. We have emphasized the unconventional phenomenology of motional narrowing in standard semiconductor quantum dots at low incident power and temperature, that makes the quantum dot emission line a sensitive probe of the extrinsic reservoir fluctuation dynamics. We have shown that the text book phenomenology of motional narrowing in nuclear magnetic resonance is recovered in QDs embedded in field-effect heterostructure. In that case, the electrical control of the QD mesoscopic environment leads to motional narrowing where the motion consists in carrier tunneling out of the defects around the QD. This effect opens the way for a protection of zero-dimensional electronic states from outside coupling through a control of motional narrowing with external experimental parameters such as a dc-gate voltage.

Acknowledgements The author gratefully acknowledges A. Berthelot, I. Favero, C. Voisin, C. Delalande, Ph. Roussignol, R. Ferreira, M. S. Skolnick and J. M. Gérard for their contribution to the experimental and theoretical works presented in this review, and G. Bastard, and P. M. Petroff for stimulating discussions.

References

1. S. Kako, C. Santori, K. Hoshino, S. Gtzinger, Y. Yamamoto, and Y. Arakawa, Nature Mater. **5**, 887 (2006).
2. C. Santori, D. Fattal, J. Vučkovic, G. Solomon, and Y. Yamamoto, Nature **419**, 594 (2002).
3. J. Bylander, I. Robert-Philip, and I. Abram, Eur. Phys. J. D **22**, 295-301 (2003).
4. X. Li, Y. Wu, D. Steel, D. Gammon, T. H. Stievater, D. S. Katzer, D. Park, C. Piermarocchi and L. J. Sham, Science **301**, 809 (2003).
5. G. Cassabois and R. Ferreira, C. R. Physique **9**, 830 (2008).
6. S. A. Empedocles, D. J. Norris, and M. G. Bawendi, Phys. Rev. Lett. **77**, 3873 (1996).
7. H. D. Robinson and B. B. Goldberg, Phys. Rev. B **61**, R5086 (2000).
8. V. Türck, S. Rodt, O. Stier, R. Heitz, R. Engelhardt, U. W. Pohl, D. Bimberg, and R. Steingrüber, Phys. Rev. B **61**, 9944 (2000).
9. R. Kubo, p. 23, in *Fluctuation, Relaxation and Resonance in Magnetic Systems*, D. Ter Haar (Oliver and Boyd, Edinburgh, 1962).
10. K. Wódkiewicz, B. W. Shore, and J. H. Eberly, J. Opt. Soc. Am. B **1**, 398 (1984).
11. A. Berthelot, G. Cassabois, C. Voisin, C. Delalande, R. Ferreira, Ph. Roussignol, J. Skiba-Szymanska, R. Kolodka, A. I. Tartakovskii, M. Hopkinson, and M. S. Skolnick, New J. Phys. **11**, 093032 (2009).
12. N. Bloembergen, E. M. Purcell, and R. V. Pound, Phys. Rev. **73**, 679 (1948).
13. A. Berthelot, I. Favero, G. Cassabois, C. Voisin, C. Delalande, Ph. Roussignol, R. Ferreira, and J. M. Gérard, Nature Phys. **2**, 759 (2006).
14. C. Kammerer, G. Cassabois, C. Voisin, M. Perrin, C. Delalande, Ph. Roussignol, and J. M. Gérard, Appl. Phys. Lett. **81**, 2737 (2002).
15. I. Favero, A. Berthelot, G. Cassabois, C. Voisin, C. Delalande, Ph. Roussignol, R. Ferreira, and J. M. Gérard, Phys. Rev. B **75**, 073308 (2007)
16. S. Seidl, M. Kroner, P. A. Dalgarno, A. Hgele, J. M. Smith, M. Ediger, B. D. Gerardot, J. M. Garcia, P. M. Petroff, K. Karrai, and R. J. Warburton, Phys. Rev. B **72**, 195339 (2005).
17. R. Oulton, J. J. Finley, A. D. Ashmore, I. S. Gregory, D. J. Mowbray, M. S. Skolnick, M. J. Steer, San-Lin Liew, M. A. Migliorato, and A. J. Cullis, Phys. Rev. B **66**, 045313 (2002).
18. P. C. Sercel, Phys. Rev. B **51**, 14532 (1995).
19. V. Karpus and V. I. Perel, Sov. JETP **64**, 1376 (1986).
20. S. W. Lin, C. Balocco, M. Missous, A. R. Peaker, and A. M. Song, Phys. Rev. B **72**, 165302 (2005).